REPORT DOCUMENTATION PAGE

Form Approved OMB No. 0704-0188

1. AGENCY USE ONLY (Leave blank)	2. REPORT DATE	3. REPORT TYPE AND DATES COVERED
	5 August 1999	Final Report

4. TITLE AND SUBTITLE

Optimal Flow Control Based on Excitation of Inherent Coherent Vortices: Fundamental Background

5. FUNDING NUMBERS

F61775-99-WE075

6. AUTHOR(S)

Dr. Nina Yurchenko

7. PERFORMING ORGANIZATION NAME(S) AND ADDRESS(ES)

R&DCFM, National Academy of Sciences
8/4 Zheliabov St.
Kiev 252057
Ukraine

8. PERFORMING ORGANIZATION REPORT NUMBER

N/A

9. SPONSORING/MONITORING AGENCY NAME(S) AND ADDRESS(ES)

EOARD
PSC 802 BOX 14
FPO 09499-0200

10. SPONSORING/MONITORING AGENCY REPORT NUMBER

SPC 99-4075

11. SUPPLEMENTARY NOTES

12a. DISTRIBUTION/AVAILABILITY STATEMENT

Approved for public release; distribution is unlimited.

12b. DISTRIBUTION CODE

A

13. ABSTRACT (Maximum 200 words)

This report results from a contract tasking R&DCFM, National Academy of Sciences as follows: The Objectives of the proposed research work are 1) Development of the fundamental ideology of the flow control (according to the Contract F61775-98-WE123) based on the generation and maintenance of a dominant type of a vortical structure (coherent vortices) with chosen values of parameters correlated with the basic flow parameters "homeopathic treatment" formula; 2) Extension of the proposed boundary-layer control method using specific temperature distribution over a surface (e.g. due to the streamwise heated strips regularly spaced in the transverse direction) to a wider range of practical applications, such as jet-flows attached to a wall of an arbitrary geometry; and 3) Studies of basic mechanisms of the vortex dynamics and essential characteristics of the evolving flow structure under the generation of large-scale coherent vortices (velocity profiles, spectral and integral characteristics).

14. SUBJECT TERMS

EOARD, Boundary Layer Control

15. NUMBER OF PAGES

27

16. PRICE CODE

N/A

17. SECURITY CLASSIFICATION OF REPORT	18. SECURITY CLASSIFICATION OF THIS PAGE	19. SECURITY CLASSIFICATION OF ABSTRACT	20. LIMITATION OF ABSTRACT
UNCLASSIFIED	UNCLASSIFIED	UNCLASSIFIED	UL

NSN 7540-01-280-5500

Standard Form 298 (Rev. 2-89)
Prescribed by ANSI Std. 239-18
298-102

EUROPEAN OFFICE OF AEROSPACE RESEARCH AND DEVELOPMENT

OPTIMAL FLOW CONTROL BASED ON EXCITATION OF INHERENT COHERENT VORTICES:

FUNDAMENTAL BACKGROUND

Contract F61775-99-WE075
5 August, 1999

FINAL REPORT
January 17, 2000

Principal Investigator: **N.F.Yurchenko**, Ph.D.

Research & Development Center of Fluid Mechanics (R&DCFM),
National Academy of Sciences of Ukraine

8/4 Zheliabov St., 252057 Kiev, UKRAINE
Tel: +38044 441-7452
Fax: +38044 216-0425
E-mail: yur@rdfm.freenet.kiev.ua

1. BACKGROUND

1. 1. Problem formulation

A variety of fluid motion of a similar type known as a streaky structure, longitudinal/Taylor/Goertler vortices, coherent vortices, etc. gives substantial evidence of certain universal peculiarities of this motion and its importance for fundamental and applied problems. It is evinced as streamwise stripes naturally visualized by sand, vapor, dust, and fish-scale of fast swimming marine animals. Although being of a speculative nature if to refer strictly to longitudinal vortices, an example of so visualized regular structure connected with a specific kind of motion is shown in Figure 1. Streamwise vortical structures are known to be an important structural element typical for various flows [20], such as

- laminar-turbulent transitional boundary layers [3, 22, 30];
- sublayers of fully developed turbulent boundary layers [4, 17, 36];
- turbulent spot environment seen as a "fringe" made from streamwise vortices;
- flows over heated or curved surfaces (affected by buoyancy or centrifugal forces) [6, 7, 20, 21, 24, 27, 31];
- rotating flows, e.g. those in a gap between concentric cylinders (Taylor vortices);
- secondary flows in curved channels and river-beds;
- MHD flows with imposed transverse forces of electro-magnetic origin;
- Langmuir circulation in ocean...

A similarly displayed form of a fluid motion may suppose its universal driving mechanisms and approaches to the study and control. Numerous computational, experimental and analytical studies

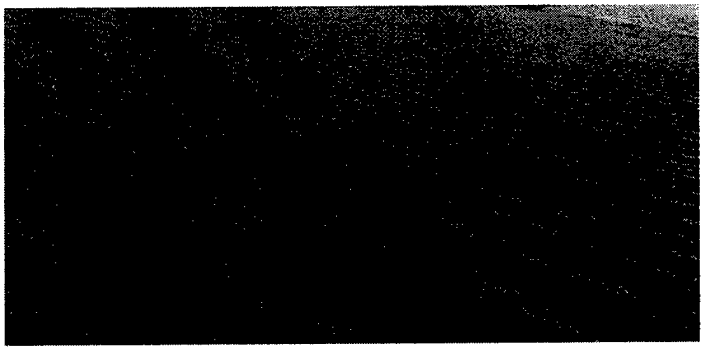

Figure 1. "Streaky" structure.

proved vortex formation and evolution to play a dominant role in producing and sustaining turbulence, i.e. processes practically important for engineering applications. Earlier investigations [20-34] demonstrated that being a deterministic flow structure, streamwise vortices are convenient and justified for detailed investigations and manipulations.

Recognized common features of vortex dynamics enabled to distinguish a group of flows, which can be studied under rigorous mathematical formulation of the problem. These are flows of viscous fluid affected by body forces (e.g. centrifugal forces or buoyancy). Balanced interaction between body forces (because of the surface curvature or its temperature different from one of the fluid) and viscous forces (because of the wall presence) gives rise to the development of streamwise vortices in boundary layers. It happens at a certain downstream position where intensities of the two corresponding vorticity sources become comparable in a process of their different individual development along a plate.

A classical case of such flows, a boundary-layer flow over a concave surface, was extensively studied in a frame of Goertler stability theory and receptivity approach [7, 20, 21, 24, 28-32]. These

fundamental studies provide an insight into the mechanisms of the vortical structure evolution and behavior. In particular, the work under the Contract F61775-98-WE123 as well as the results published in [26, 31] yielded a detailed picture of natural (unforced) emergence and evolution of streamwise vortices in boundary layers affected by centrifugal (body) forces, i.e. in flows where they are an intrinsic vortical structure. Besides, selection of virtual space-scales of fluid motion after the vortices were generated with a given scale; vortex scale transformation downstream and across boundary layer were considered with an emphasis to possible applications of the obtained fundamental results.

It should be taken into account that in practice, engineering devices mostly operate in turbulent environment. And what is more, such flows often contain inherent coherent vortices. In particular, low-speed streaks related to the turbulence production were found to be similar to the vortical structure characteristic for a pre-turbulent stage of laminar-turbulent transition [3, 4, 17]. This structure dynamics and its role in fluid transport near a wall were also successfully analyzed using the stability approach [36].

Thus, natural self-organization and evolution of streamwise vortices is what unifies many flows different by their physical origin. It defines the present problem formulation focused on studies of streamwise vortices under conditions of the laminar flow transition to turbulence up to fully turbulent boundary layers. The cases of transitional and turbulent boundary layers over concave surfaces as well as the near-wall flows of a turbulent boundary layer are notable for their dominant intrinsic streamwise vortical structure.

More generally, the task can be formulated as one based on a ***flow control similarity principle***: **specific generation of a vortical structure similar to one intrinsic to the flow and naturally dominating under certain conditions.**

It is supposed to provide an optimal surface-flow interaction from a viewpoint of energy outlay as well as convenience and flexibility of the flow management. Practically, it means

(1) establishment of typical features and scales of vortical motion for a set of basic flow parameters of interest;

(2) controllable stimulation of the vortical motion of a similar type but of different scale and intensity depending on problem parameters and objectives.

In other words, the generally formulated problem and its solution starting from transitional to fully developed turbulent boundary layers can be considered as a basis for searching optimal ways of boundary-layer control through its inherent structure manipulation. It means the development of a soft way to controllably vary fluid motion space-time scales and, accordingly, its transport properties without drastic changes of the vortex dynamics.

Fundamental objective of the present work is the application of the formulated similarity principle related to streamwise vortices to control properties of both transitional and turbulent boundary layers.

Transitional boundary layers due to their larger scales (compared, e.g. to viscous sublayers) and more definite deterministic investigation methods give a possibility to study in detail evolution of streamwise vortices generated with a given scale in transitional boundary layers. Here, thorough combined experimental/numerical studies make it possible to get details of the vortical flow evolution in a form of its structure (flow topology) modification depending on basic flow parameters and values of the forcing factors. Basic knowledge of the vortex dynamics mechanisms driving natural and forced development of boundary layers must bring a most elegant solution to control a given flow as well as ideas to apply this solution to similar flow situations.

To link the fundamental approach with practical needs, it is reasonable to extend the methods, results and their interpretation to a fully developed turbulent boundary layer where an organized vortical structure is initiated and maintained in a near-wall region. In addition to presentation of flow topology and kinematic characteristics, such as transverse U-velocity profiles, both parts of the investigation are

described in spectral terms which allow to see new aspects of the phenomena due to deeper interpretation of the obtained results.

1. 2. Spectral description of boundary layers with embedded large-scale eddies

Last 20 years brought satisfactory results in mathematical modeling of turbulent flows, i. e. in adequate description and reliable computation of this complex physical phenomenon. Now engineering models of turbulent transfer based on single-point closure models (for example, the well-known k-ε model) are widely used and allow to obtain statistical information about the turbulent structure of investigated flows satisfactory for many practical applications [15, 16]. However in case of available large-scale eddy structures (LSES), these models fail to give though a qualitatively proper picture of turbulent momentum, heat and mass transfer. Long lifetimes of LSES cause a fluid (or admixture) particle, trapped by such an eddy field, to be transported to significant distances without a noticeable change of direction. Schematically, it is illustrated in Figure 2.

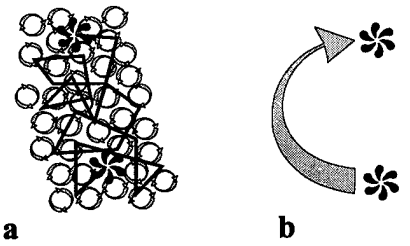

Figure 2. Fluid transport patterns in vortical fields of
(a) homogeneous turbulence and
(b) one with embedded large-scale vortices

This feature disagrees with postulates of Euler's K-theory of turbulence diffusion where the turbulent transfer is considered by analogy with the Brownian motion, that is a randomly wandering process. As a consequence, fluid transfer by LSES cannot be described in the framework of standard turbulence models of a gradient type [14]. Coherent structures were also shown to affect the PDF distribution displaying its essentially non-Gaussian form with substantial values of asymmetry and excess coefficients [16]. Therefore, effect of LSES on flow dynamics in no case can be neglected.
Latest research results on modeling of non-local turbulent transfer in impinging jets [1], in convective atmospheric boundary layers [8] and in free and near-wall shear flows [9, 10] confirm the dominating role of available LSES in transport properties of various flows.

In spectral terms, the role of large-scale vortices in fluid transport near a wall is recognized due to their basic contribution to the long-wave "energy-carrying" part of the turbulent kinetic energy spectrum. The mechanism of turbulent kinetic-energy redistribution between a long-wave region and the inertial interval of turbulent fluctuations is important to study with regard to the effect of "choking" of the spectral energy flux by quasi-2D LSES. These studies enable to formulate basic principles of turbulent transfer control. Being combined with deterministic investigations of a streamwise vortical system, they can yield generalized fundamental background and practical recommendations concerning effective control of flows with large-scale vortical structures.

For explicitness, a typical spectrum of turbulent fluctuations is shown in Figure 3.
Nowadays, validity of Kolmogoroff's hypothesis about a locally isotropic structure of small-scale turbulence in the inertial interval of the turbulent spectrum is practically unquestionable. Statistical structure of this spectrum interval is described with good accuracy by the equilibrium PDF, i.e. a motion of fluid particles in the field of isotropic turbulence can be characterized as a Brownian motion (diffusion).

Short-wave part of the spectrum corresponds to dissipation scales of turbulence. It is a part of comparatively low kinetic energy which transforms into heat by viscosity action. Here, turbulent fluctuations have a complicated statistical structure characterized by considerable values of asymmetry and excess coefficients (with strongly pronounced non-Gaussian distribution). However

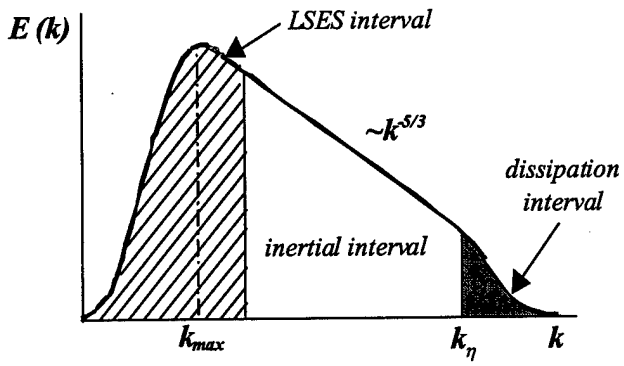

Figure 3. Spectrum of turbulent fluctuations:
$k_{max} \sim 1/L$, $k_\eta \sim 1/\eta$;
L - flow lengthscale, η - Kolmogoroff's lengthscale,
$L >> \eta$ *at* $Re >> 1$

these effects are negligible for processes of turbulent transfer while turbulent flows are modeled using a method of statistical moments. In case of developed turbulence, a rate of viscous dissipation equals with good accuracy to the spectral flux of turbulence energy; therefore it is not necessary to consider here a complicated statistical structure of small-scale turbulence.

The energy interval of long-wave fluctuations (large-scale vortices), on the contrary, contains a main part of turbulent energy and is dominating in processes and character of turbulent transfer. Long-wave fluctuations (LSES) are characterized by a comparatively large time of relaxation and carry information about a history and structure of an averaged flow (memory effects). This spectrum region is usually anisotropic and PDF (being considerably non-Gaussian one) is described by high values of the mentioned coefficients.

Thus, fluctuations contributing to the energetic and inertial intervals of the spectrum (or vortices of corresponding scales) should be main objects of turbulent flow modeling as well as of studies dealt with further applications of fundamental results.
Analysis of spectral properties of bounded flows with embedded large-scale vortices both in laminar and turbulent environment should bring more details and better understanding of vortical structure evolution under natural and controlled conditions. In its turn, insight into the vortex dynamics must reveal optimal ways/techniques to interfere the process so that to sustain a favorable structure for a formulated flow control purpose (heat transfer enhancement, boundary-layer transition or separation delay). Mechanisms of the spectral energy choking by quasi-two-dimensional LSES, i.e. specific transfer of turbulent kinetic energy from a long-wave towards inertial region of the turbulent spectrum, must help to formulate principles of effective turbulent transport control.

In addition to practical orientation of the research, the formulated approach and expected results must contribute to the development of proper turbulence models, adequate mathematical descriptions of turbulent momentum, heat and mass transfer using, in particular, large-eddy simulation tools. Advanced theory will make it possible to extend the developed methods to solution of a wider range of practical problems, e.g. control of impinging jets, through prediction of the large-scale dynamics at high Reynolds numbers.

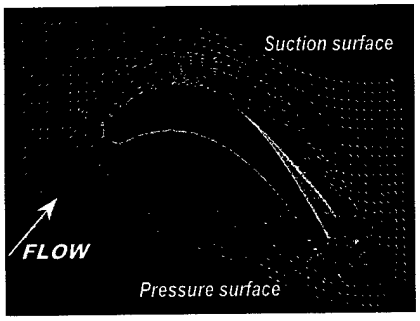

Figure 4. Velocity field pattern around a low-pressure turbine blade; 1/2 cascade passage [18]

1. 3. Connection to applications (low-pressure turbine blade)

A key point of the present investigations is generation of streamwise vortices with given parameters in a flow where this type of motion is inherent, i.e. in boundary layers affected by body forces. The present formulation of the problem originated from a practical need to improve flow conditions around a low-pressure turbine blade. First of all, it deals with the development of a simple and reliable method to control flow separation on a suction side of the blade. Figure 4 illustrates the configuration of the flow field around a low-pressure turbine blade showing a position of a separation bubble on its surface [18].

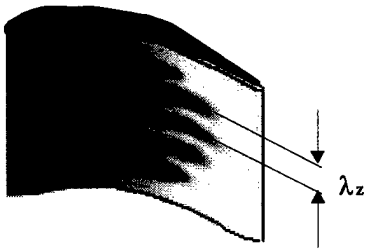

Figure 5. Visualized streamwise vortical structure on a pressure side of a low-pressure turbine blade [18, 27]

To estimate space-scales of a vortical motion in a boundary layer over the turbine blade that can be taken as a reference value for the flow control purposes, one can assume it to be of the order of a regular LSES found due to liquid crystal visualization on its pressure side. Figure 5 gives an idea about this naturally self-organized streamwise vortical structure arising at Re_C =67500 with a scale λ_z=8 mm (Re_C is a cord-based Reynolds number). Analysis of the boundary-layer vortex dynamics in the frame of Goertler stability theory explained physical mechanisms of the vortical structure formation [32] and led to the present formulation of further studies of a boundary layer over a concave wall aimed, in particular, to flow separation delay on a suction side of the turbine blade.

2. METHODS, FACILITIES, ARRANGEMENT OF INVESTIGATION

2.1. Experimental setup, methods of flow field registration –

are basically the same as described in the Final Report on the Contract F61775-98-WE123 and partly presented in the published papers [6, 25-27, 29, 31, 32]. Depending on the research purpose and experimental convenience, vortices were generated using three ways as shown in Figure 6 together with a general sketch of the investigation approach [23, 28].

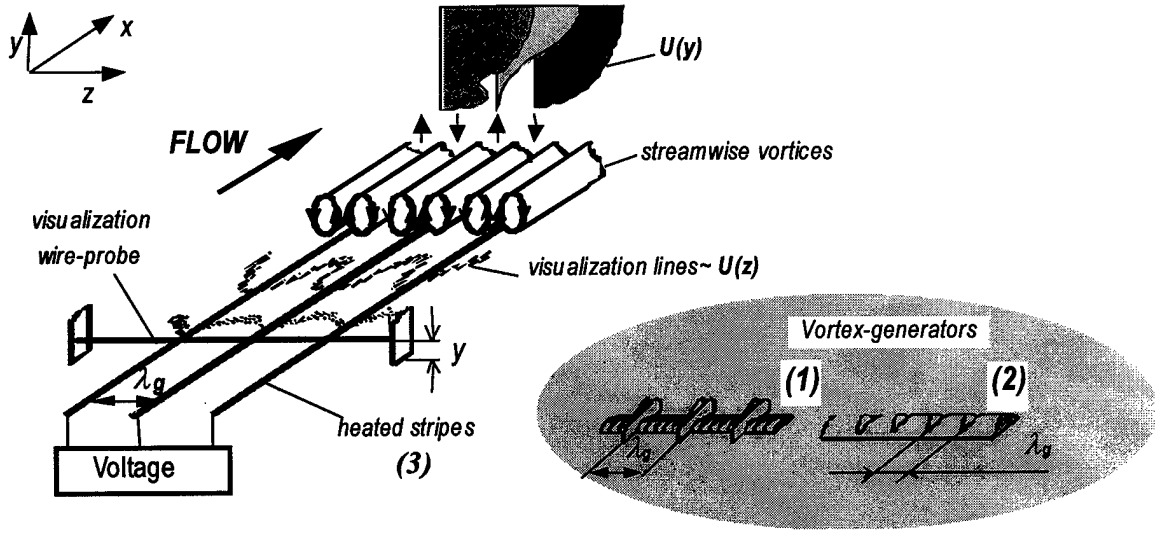

Figure 6. Sketch of the experiments and velocity fields of boundary layers with generated streamwise vortices

For spectral analysis of a boundary layer, mechanical vortex-generators of various sizes were used. A vortex-generator array was placed normally to the velocity vector on a test surface, effective height of vortex generators having been 3, 5 and 7 mm. A distance, λ_g, between adjacent vortex generators defined a scale of the vortical structure induced in a boundary layer. Changing this scale, one could see a different boundary-layer response (receptivity) to a scale of generated vortices. Electrochemical flow-field visualization in xz-plane provided express-information about this response in a form of

$U(z)$ velocity profiles, showing vortices of the same, $\lambda_z=\lambda_g$, or modified scale depending on correlation between λ_g and basic flow parameters.

Experimental studies of a boundary-layer spectral response to generated streamwise vortices were carried out in a low-turbulent water channel described in [28]. Its open test section was of *10 x 25 x 300 cm,* a free-stream velocity range, U_0=0.05-0.6 m/s, or typical length-based Reynolds numbers, Re=(0.6-1.4)·10^5. The studied boundary layer developed on its changeable (reinstalled) bottom, *25 x 300 cm*, which could be flat or contain a concave section (curvature radii, R = *1.0, 4.0* and *12 m*). The concave surface case, i.e. the boundary-layer flow under centrifugal forces, allowed analyze the problem in the Goertler stability approach. Scales of generated streamwise vortices covered a range from neutral to most amplified vortices according to the Goertler diagram.

In addition to flow visualization, hot-wire measurements were carried out (using one-component probes of a DISA system) at U_0=0.1, 0.2 and 0.6 m/s that enabled to get spectral characteristics of the boundary layer. These flow conditions corresponded to subsequent stages of the natural laminar-turbulent transition manifested in a form of propagating Tollmien-Schlichting waves, formation of streamwise vortices and their breakdown to turbulence. Hot-wire probes fixed at y=4mm from a test surface and at Δx=5 cm downstream of the vortex-generator array, i.e. in a region of the most intense interaction of natural and generated disturbances. Both normal velocity profiles (as those shown in Figure 5) and spectral characteristics were measured at three spanwise positions along λ_g corresponding to downwash (z= 0) and upwash (z=λ_g/2) interfaces between neighboring vortices and between these two positions (z=λ_g/4).

2.2. Numerical approach

Formulation of the ***numerical problem*** was matched with the experimental one as it was described in the Final Report on Contract F61775-98-WE123, as well as in [25, 26].

Numerical modeling was based on a code developed for the direct numerical simulation (DNS) of a laminar-turbulent transition in compressible subsonic boundary layers; here, it was applied with the inclusion of body force terms into the Navier-Srokes equations. To reveal physical mechanisms of the studied phenomena, Goertler stability theory [21] was assumed as a basis. The stability diagram (Figure 7) was used as a reference for the scale choice of induced vortices, prediction and interpretation of their behavior. DNS were carried out for a Goertler number of Go_d =*15,* and a Reynolds number of Re_d=*595*, where both parameters are based on the Blasius reference length $d=(\nu_o x / U_o)^{1/2}$. The spatial dimensions are referenced to the same length, and time is non-dimensionalized with d/U_o. The free-stream Mach number considered is M=*0.8*, the free-stream temperature is T_o=*290 °K*, the medium is air with constant isentropic exponent γ=*1.4* and Prandtl number P=*0.71*. The momentum thickness based on this profile is ϑ =*0.66 d*, such that a corresponding Goertler number based on ϑ is Go_ϑ=*8*. The fundamental in the spanwise direction was taken to be α_z=*0.66,* corresponding to Λ=*236*, i.e. from the range of most amplified disturbance wavelengths according to the Goertler diagram. Then the second harmonic corresponds to Λ=*84* staying still in the domain of amplified wavelengths, while all further harmonics are linearly damped.

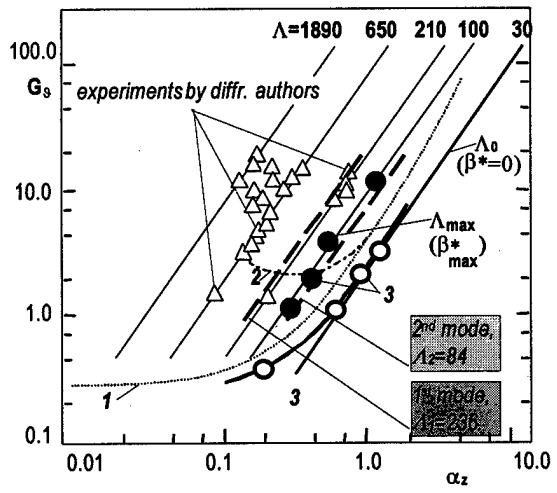

Figure 7. Goertler diagram ($G_\vartheta=\vartheta^{3/2} U_0\nu^{-1}R^{-1/2}$, $\alpha_z=2\pi/\lambda_z$): neutral curves by Floryan & Saric (1982) -1, Hall (1983) –2; Λ_0 and Λ_{max} - experimental curves for vortices with zero and maximum (Λ_1≈100) growth rates [30]; 1st and 2nd modes considered in the numerical simulation

Briefly, the approach to both numerical and experimental studies of generated streamwise vortices consists in their thermal excitation using streamwise flush-mounted heated stripes regularly spaced along z (Figure 6, position 3). The main issue is formulated as a constant boundary condition in a form of a z-periodic temperature gradient $\Delta T(z)$. The introduction of only a temperature disturbance required the vortex system to self-establish without any pre-determination except for the imposed spatial scale in the spanwise direction.
Such forced development of streamwise vortices was analyzed for two cases of boundary conditions (different scales, λ_g, of generated vortices) considered as *Cases 1* and *2*.

Case 1 describes excitation of a purely second mode with a non-dimensional vortex scale Λ=84 linearly amplified according to the Goertler stability diagram, and harmonics thereof (see Figure 7).

Case 2 corresponds to generation of a slightly irregular vortical structure that means additional stimulation of the most amplified first mode, Λ=236. Practically, *Case 2* was realized due to one of the heated stripes insignificantly shifted along z, thus modeling to some extent imperfectness of experimental conditions or applications of the method in practice.

Case 0 is taken as a reference to the thermally forced cases to see unforced evolution of Goertler vortices without any permanent forcing at the wall. The wall was homogeneously kept thermally perfectly insulated. A very small initial pulse disturbance was introduced to keep the system in the linear regime for a very long phase. In this way, "generic" Goertler vortices could arise, free of any transients.

3. RESULTS AND DISCUSSION

3.1. Generation of streamwise vortices in boundary layers – development of separate modes and overall flow topology

To get an insight into vortex dynamics under conditions of streamwise vortical structure generation, first of all, natural evolution of the vortices from their emergence to breakdown in a process of a laminar-turbulent transition was analyzed. It was described in detail in the Final Report on Contract F61775-98-WE123. Good agreement was found between numerical and experimental results resumed in a form of a sequence of flow field patterns taken during the evolution process (Figure 8, case 0). It is typical that in the very beginning of the vortical system formation, the overall vortex size and the vertical position of the vortex core remain constant. This stage is followed by rapid growth of the vertical scale of the vortices and, consequently, by the development of strong shear layers separating adjacent counter-rotating vortices. Finally it results in the breakdown of this initial vortical system and formation of a new one with different space scales.

Like in case of natural vortex evolution, the process of the *forced vortex development* passed through the emergence- and growth phases to the vortical system breakdown. Figure 10 shows the downstream scale-transformation during these phases as a sequence of flow-field patterns in a form of iso-velocity $U(z)$ contour maps across a boundary layer and flow topology (stream-traces in the plane normal to the flow direction).

For systematic and complete analysis, the results are discussed following four successive parts corresponding the successive phases of the vortical system development under different forcing conditions: 3.1.1: Vortex emergence, 3.1.2: Vortex growth 3.1.3: Vortex breakdown, 3.1.4: Vortex system post-breakdown. During the discussion of each case (0, 1, 2) multiple references will be made to two types of the results:

a) temporal (or respectively, streamwise in experiments) evolution of amplitudes of separate modes, that are constituents of all flow variables (12 spanwise modes were used for the computations),
b) mentioned above contour maps of the velocity components in y-z-plane (vortical system cross section) at various stages of their evolution.

Here, mode-amplitude of the k^{th} mode, $|\hat{U}|_k$, of the flow variable U means $|\hat{U}|_k = (_0 |\hat{U}_k(y)|^2 \, dy)^{1/2}$. Thus, $|\hat{U}|^2_k$ is a measure of y-averaged energy, contained in each of the modes of the signal U^2 such that the sum $|\hat{U}|^2_k$ over all k 0 represents the y-averaged mean square value of the flow disturbance.

3.1.1. VORTEX EMERGENCE --

a phase between initiation of disturbances until the moment when a saturated level of the mode-amplitudes is established.

Here, initial disturbance transients decay, preferred signal components are selected by the flow and transformed into amplifying components of the evolving vortex system. Depending on the forcing or a magnitude of the initial perturbations, the transient phase may be followed by a mode evolution due to linear instability mechanism, i.e. exponential growth of mode amplitudes downstream (or in time). Figure 8 shows the evolution (*Case 0*) of the logarithmic amplitudes of the $k=1,...,12$ modes $|\hat{U}|_k$ for all the flow variables U, i.e. the momentum in streamwise, spanwise and normal directions m_1, m_2, m_3 as well as specific volume v and total energy e.

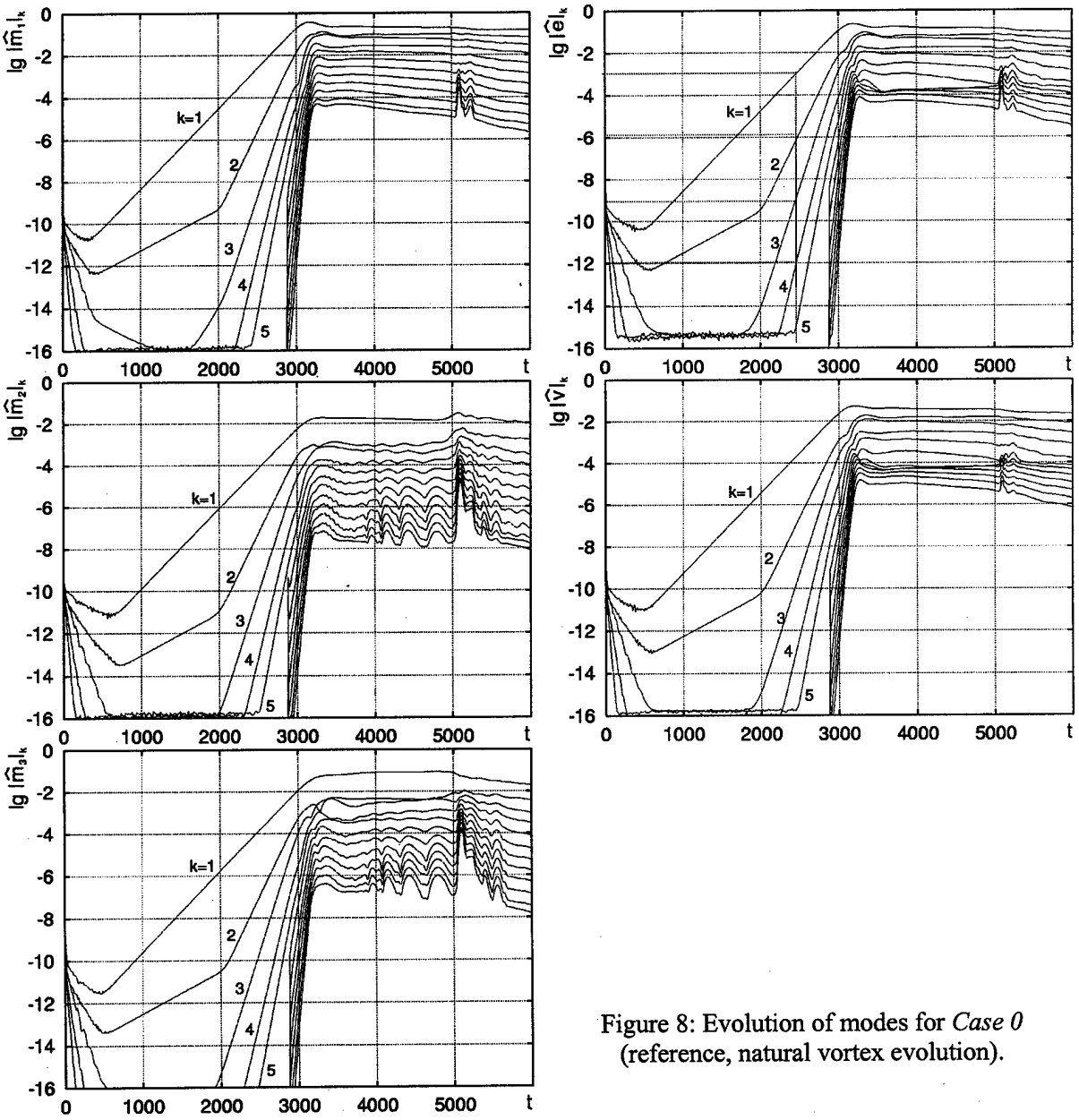

Figure 8: Evolution of modes for *Case 0* (reference, natural vortex evolution).

Case 0. The mode development displays at least four distinct phases, of which the first one is to be discussed here. The emergence phase ranges from $t=0$ to about $t=3200$. The simulation, as can be seen, started with very low amplitudes. After initial oscillations, all transients stayed under amplitudes of 10^{-10}. Correspondingly, the most amplified mode (fundamental, $k=1$) accumulates energy most rapidly compared to all the other modes. As long as its amplitude remains very small, the other modes behave as predicted by linear stability theory. In particular, after a short transient, the second mode starts growing too (though weaker than the fundamental) as it is in the range of unstable wave numbers in the Goertler diagram. All other modes are linearly damped, and so they decay down to the round-off level of the computer (double precision 10^{16}). Since the fundamental, $k=1$, rapidly acquires an essentially larger amplitude than other modes, the amplitude evolution of all higher modes couples it. It happens due to the generic, quadratic nonlinearity of the Navier-Stokes equations (or rather the convective acceleration term), since it correlates the amplitudes of the higher harmonics $|\hat{U}|_k$ and of the fundamental "driving", , mode in a simple way: $|\hat{U}|_k \sim (|\hat{U}|_1)^k$.

This fact is illustrated by blue dotted lines on the total energy plot, Figure 8, showing mode amplitudes correlated with the first mode, $k=1 \rightarrow |\hat{U}|_1=10^{-3}$ and correspondingly: $k=2 \rightarrow |\hat{U}|_2=10^{-6}$, $k=3 \rightarrow |\hat{U}|_3=10^{-9}$, $k=4 \rightarrow |\hat{U}|_4=10^{-12}$.

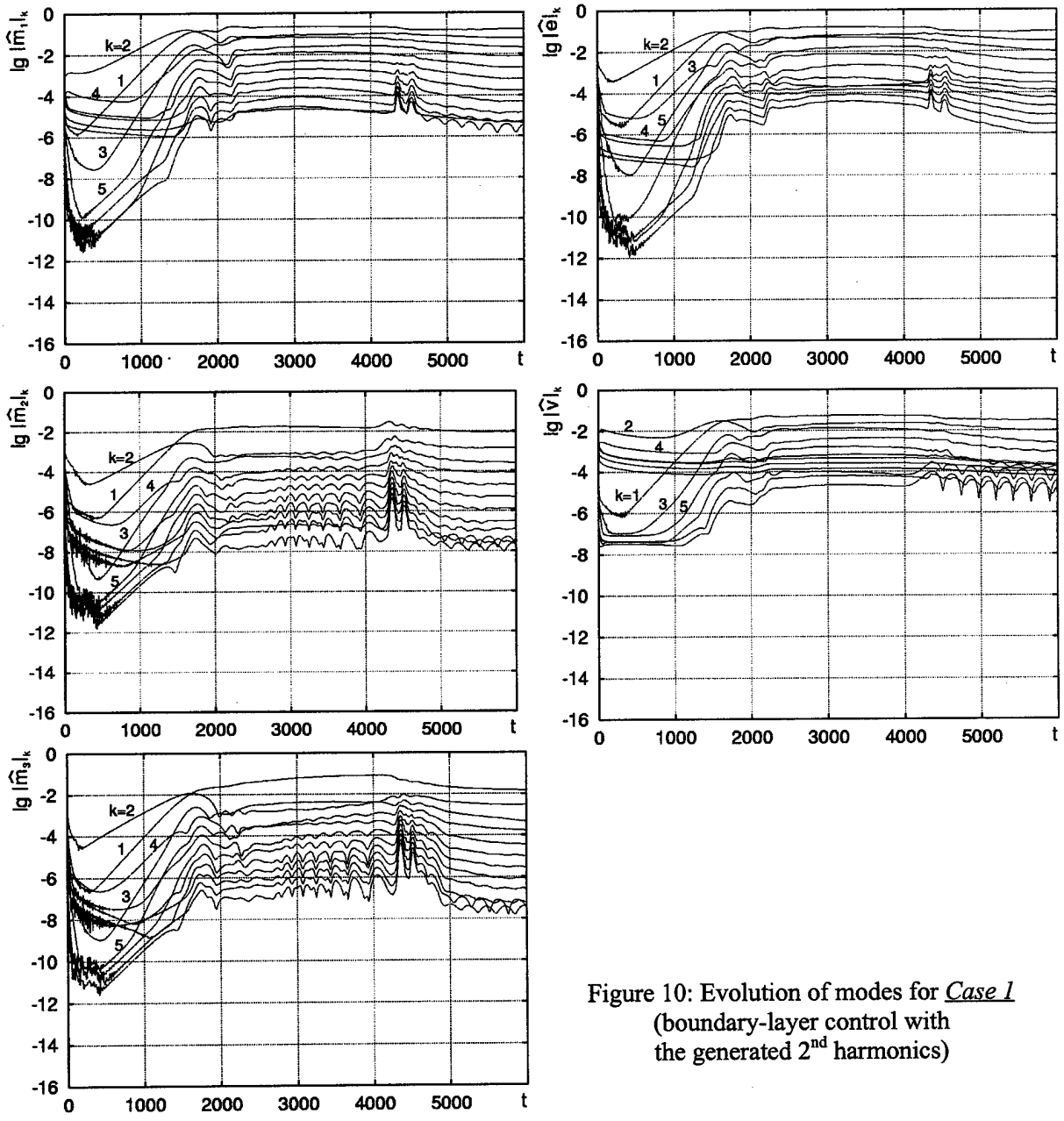

Figure 10: Evolution of modes for *Case 1* (boundary-layer control with the generated 2nd harmonics)

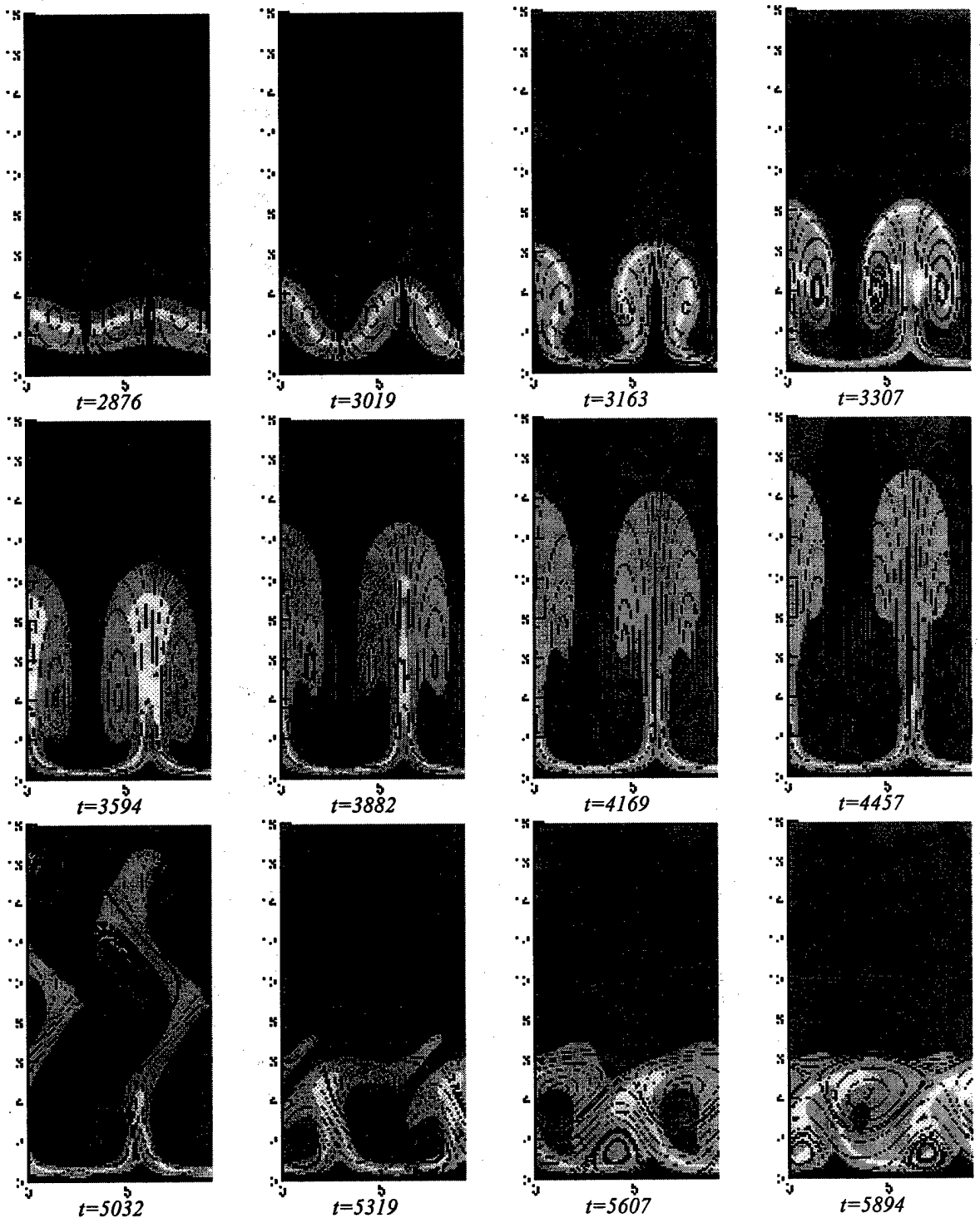
t=2876
t=3019
t=3163
t=3307
t=3594
t=3882
t=4169
t=4457
t=5032
t=5319
t=5607
t=5894

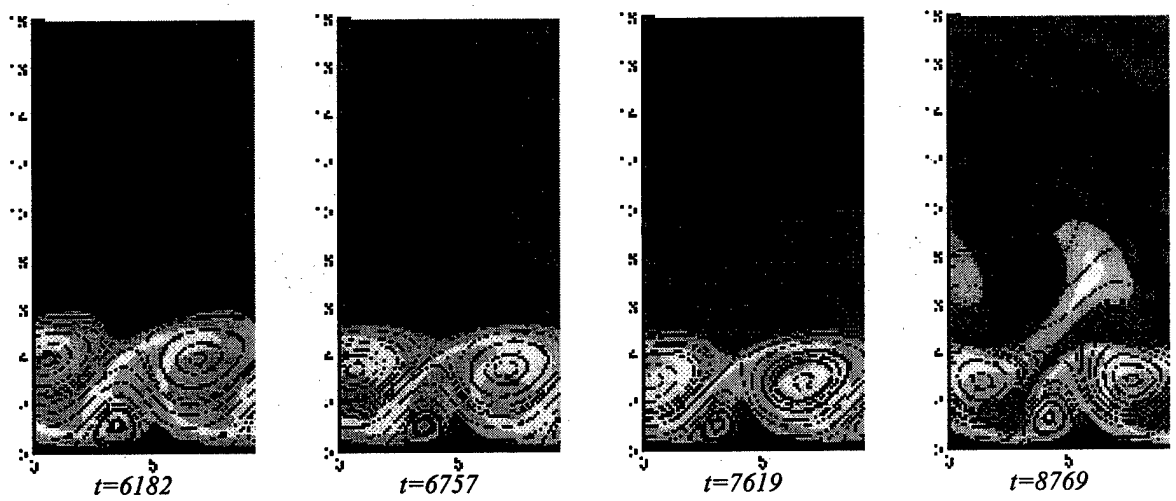

Figure 9: Evolution of vortex structure in *Case 0*:

Vertical=wall normal direction y, horizontal=spanwise direction z.

In the logarithmic plot, it results not only in a characteristic, constant vertical spacing from mode to mode, but also defines a slope of separate curves. Indeed, since the first mode grows exponentially according to the Goertler diagram, its amplitude is presented by a straight line with a slope corresponding to the respective amplification rate. And due to the described driving mechanism of the first mode with respect to the higher modes, their amplitudes evolve along straight lines with a slope being an integer multiple of the growth rate of the fundamental mode. It is important to note, that this mode structure of the higher harmonics is determined solely by the most amplified first mode rather than by their own individual behavior due to linear dynamics, even though the overall disturbance levels are extremely small at this stage. In this sense, the simulation of *Case 0* can be considered as displaying the emergence of inherent streamwise vortices. The corresponding vortical structure is shown in the first three patterns of Figure 9. It should be mentioned, that the first mode follows its eigen-behavior for so long, that the mean velocity profile is getting already quite distorted at $t=3163$ (see contour lines of $u=v\ m_1$ in Figure 9). One obvious feature of the vortex emergence phase is invariance of the overall size of vortices and their vertical position in spite of all mode-amplitudes increasing.

The *emergence of streamwise vortices under controlled conditions* is less regular compared to the above analyzed *Case 0* because finite amplitude transients appear due to the more realistic sudden switch of the small, but finite thermal forcing at the wall.

The initiation of the vortex system in *Case 1* occurs primarily due to pure second harmonic forcing (wall temperature disturbance, containing components of 2^{nd}, 4^{th}, 6^{th}, 8^{th}, 10^{th} and 12^{th} modes). This is clearly displayed in Figure 10 by the mode structure for times up to about $t=500$. Naturally the even-odd mode decoupling is best seen in the plot for the specific volume v. It is interesting to mention that the initially very small, suppressed, fundamental mode is able to follow its eigen-behavior, i.e. to grow faster than the second mode before reaching the saturation state.
Thus, it can be concluded, that the feedback from the higher modes to the first mode seems to be very weak. The result of this mode-competition (even-odd) can be seen again in the flow topology patterns (No. 1 and 2) of Figure 11. The emergence phase (including the formation of the dominant larger scale vortices) in this case is finished at a time $t\approx1800$.

Case 2, realized due to a slight shift of one of the thermal stripes of *Case 1*, means a weak forcing of a fundamental mode additionally to the even-mode forcing of *Case 1*. Although again here, like in

Case 1, the second mode has a larger initial amplitude than the fundamental (see Figure 12), the first mode takes over very rapidly and leads the vortex system into saturation extremely fast. As a result, the emergence phase is over at $t \approx 1100$. The first pattern of Figure 13 shows, that at the very end of the emergence phase of *Case 2*, a similar vortex system is established as at $t \approx 3300$ in case 0 (see pattern 4, of Figure 9).

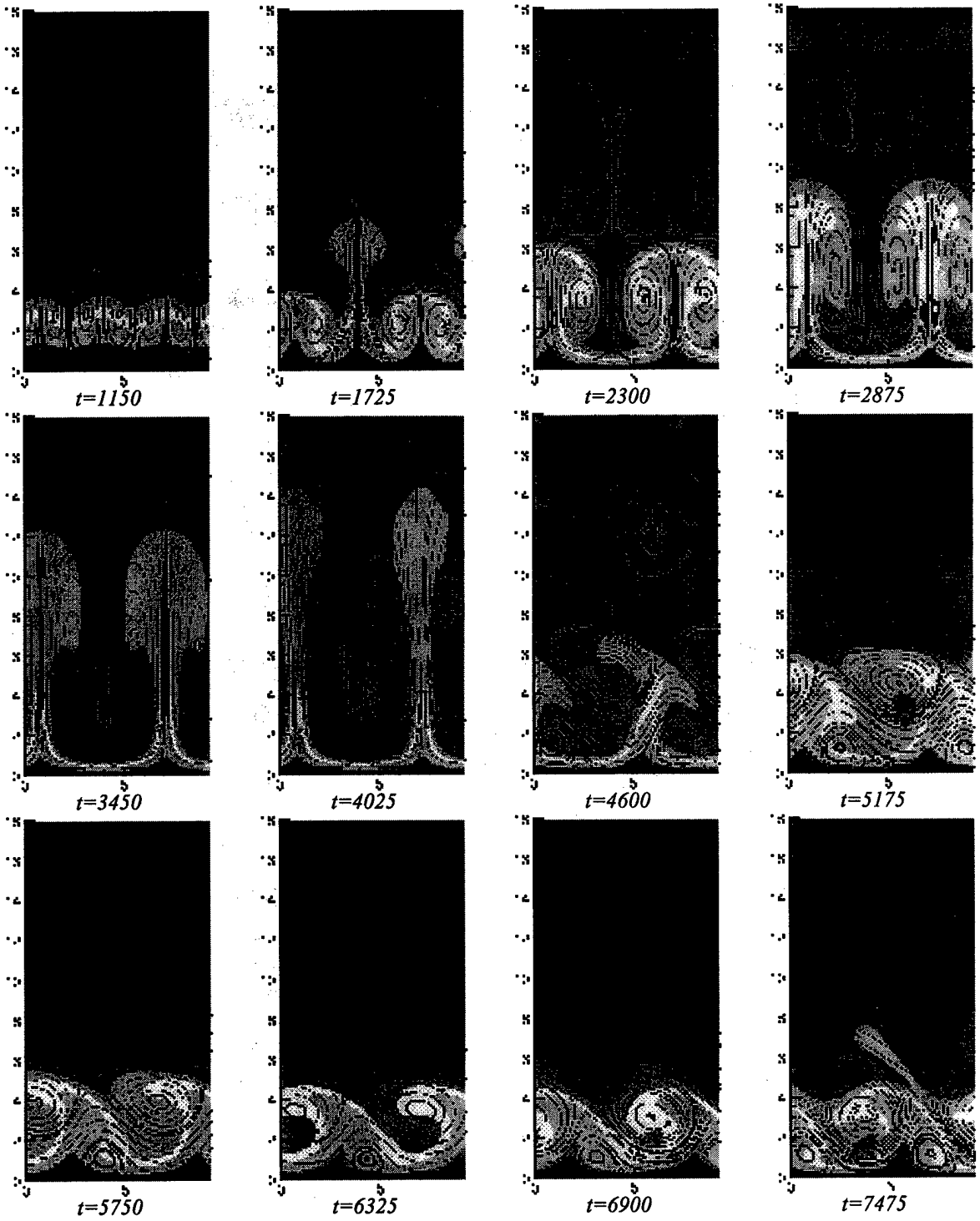

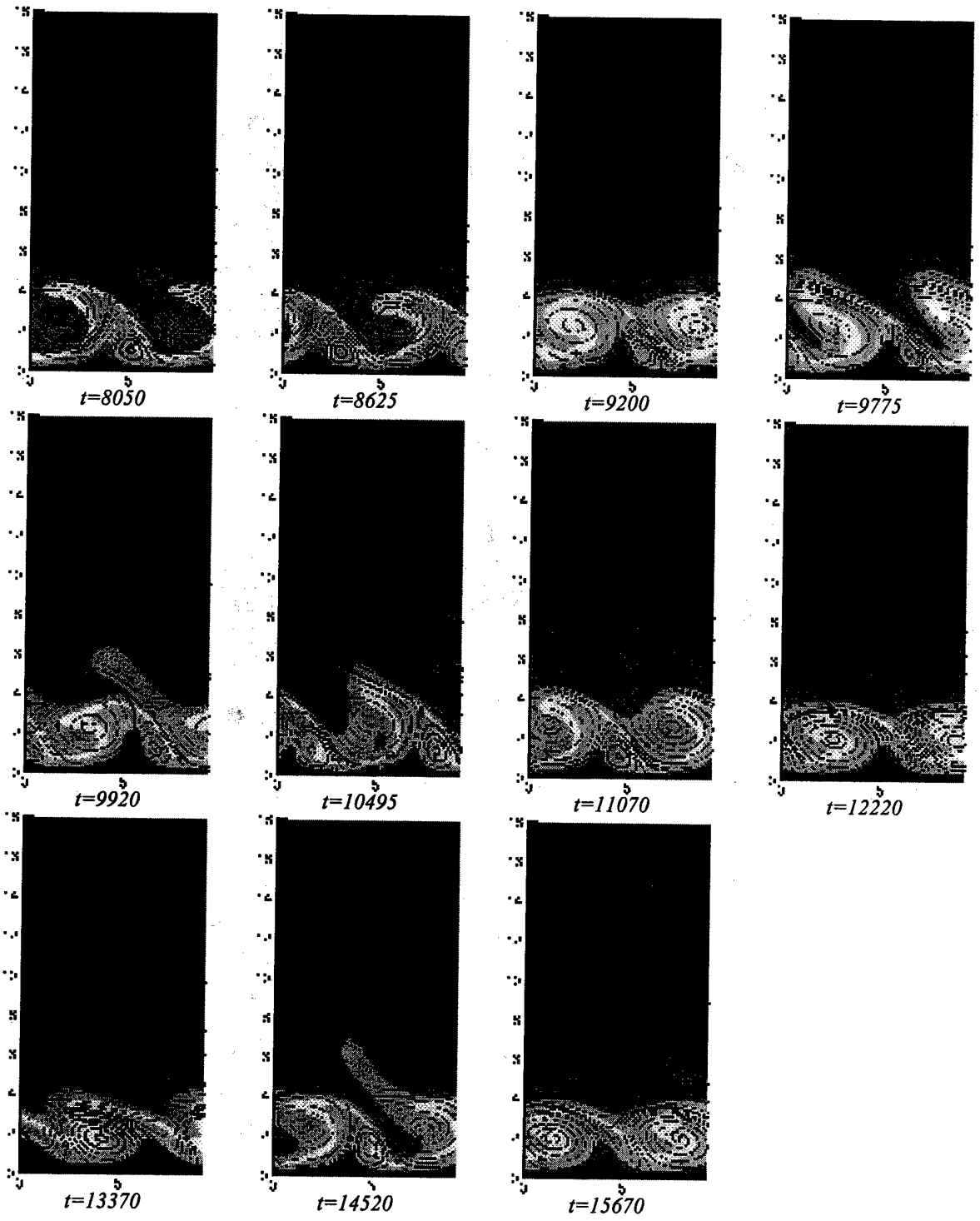

Figure 11: Evolution of vortex structure in *Case 1*:
Vertical=wall normal direction y, horizontal=spanwise direction z.

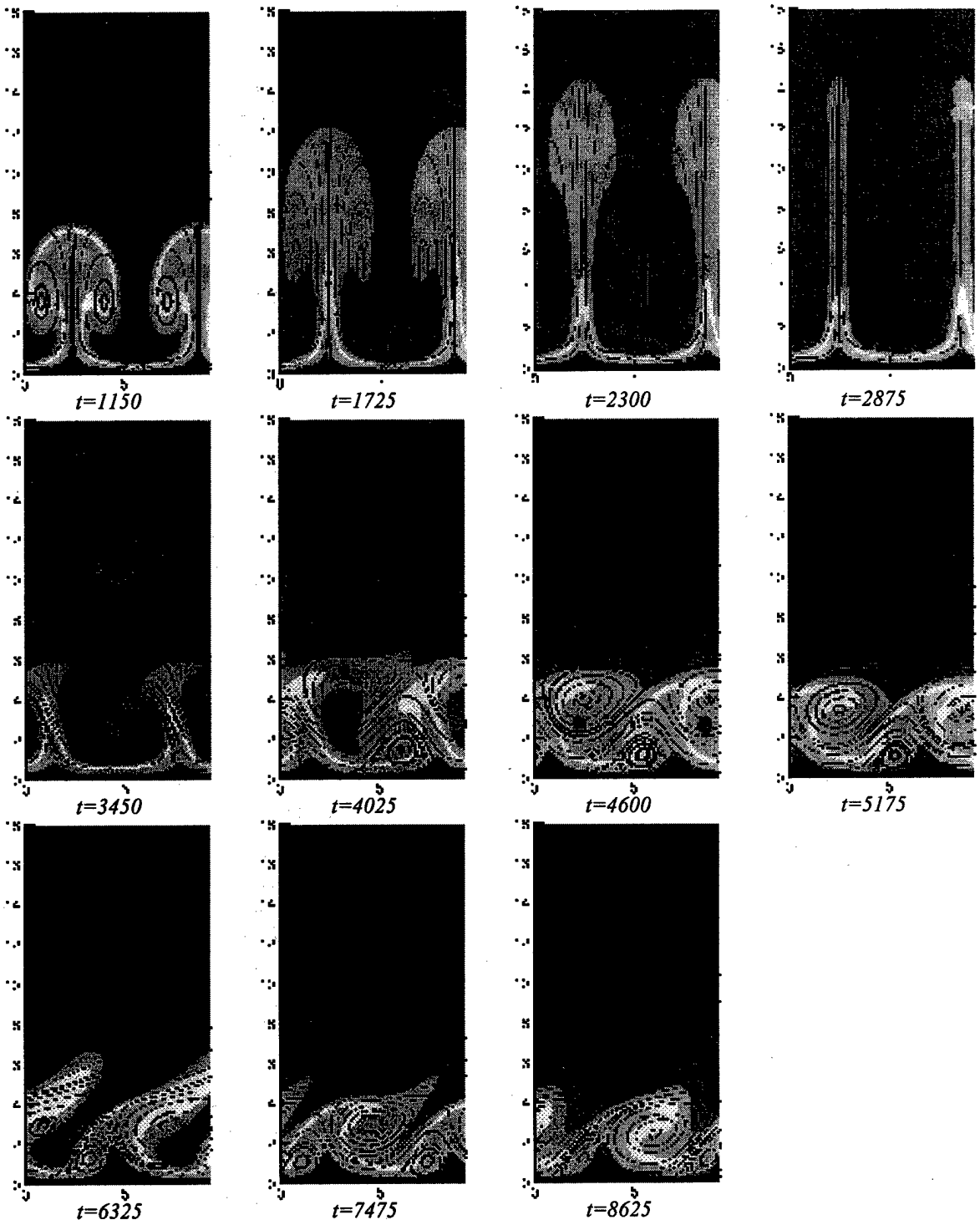

Figure 13: Evolution of vortex structure in *Case 2*:
Vertical=wall normal direction *y*, horizontal=spanwise direction *z*.

3.1.2. VORTEX GROWTH --

is a phase of the vortical structure development with all mode amplitudes saturated.
Thus during this phase, energy is only non-linearly re-distributed between the modes, whereas in the emergence-phase a continuous increase of mode energy was observed. The vortex growth phase is very important from the viewpoint of flow control, since it is characterized by a well developed, stable vortex system which can be used e.g. for separation delay due to enhanced mixing of streamwise momentum by large scale "energetic" vortices.
Therefore basic analysis of this phase is necessary to understand why and when it ends with an overall collapse of the vortices, what and how should be done to maintain the favorable vortical system as long as possible.

Case 0. Evolution of saturated mode amplitudes for the unforced, natural vortex development is shown in the mode diagrams of Figure 8. The growth phase extends from $t \approx 3200$ to $t \approx 5000$, i.e. along $t_0 = 1800$. Several interesting and typical features of the mode-amplitude behavior can be noted here. The most striking one, seen in the mode diagrams of all variables is the very end of the phase, marked

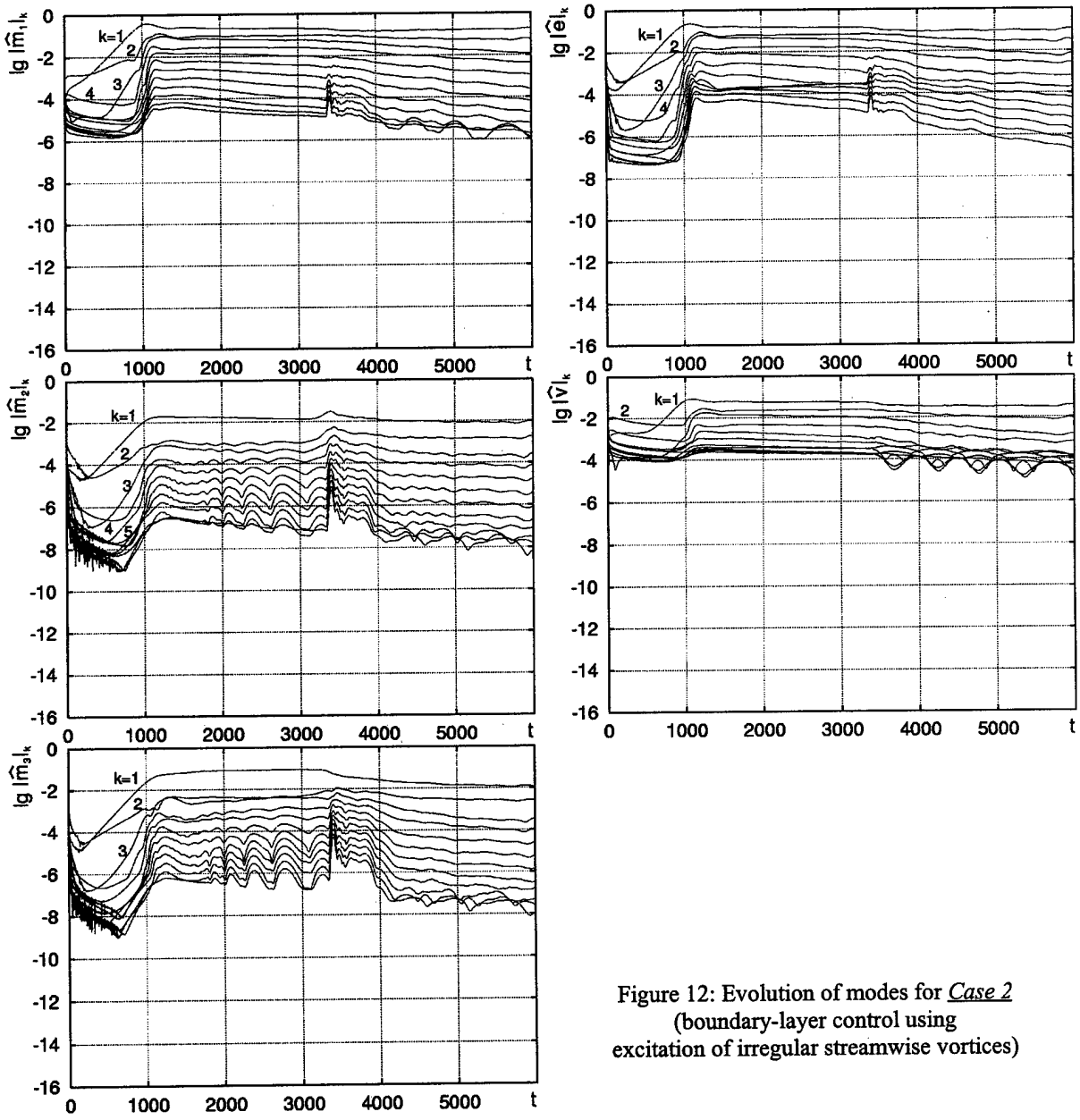

Figure 12: Evolution of modes for *Case 2* (boundary-layer control using excitation of irregular streamwise vortices)

by characteristic spike signals, primarily in the high order modes. The appearance of these spikes gives an evidence of the vortex system breakdown.
Another feature is, that a sequential built-up of the breakdown event can be observed exclusively in the m_2- and the m_3-modes, while the other flow variables experience a sudden spike out of an otherwise "well-established" and almost invariant previous mode structure. This is an indication of the started vortex breakdown, namely some instability of the spanwise and normal momentum (velocity) component field. The 4 to 8 patterns of Figure 9 show a sequence of snapshots of the vortical structure in the vortex growth phase. While the vortex shape stayed invariant for a long time during the emergence phase (patterns 1-3, Figure 9), the onset of the vortex growth phase is recognized by an almost time-linear vortex elongation in the wall normal (y) direction. Accompanied by this growth, an elevation of vortex centers over a wall is observed from about half the original boundary layer thickness to a height well beyond the original boundary layer thickness. The vortices extend far into the free-stream thus transporting high x-momentum fluid into regions close to the wall.

Cases 1 and 2.
Effect of heated longitudinal stripes on the vortex system evolution can be seen in the mode-diagrams, Figures 10 and 12. Although general mode-structure behavior is qualitatively similar to that of the reference *Case 0*, one essential quantitative difference can be deduced from the figures: the vortex growth phase is certainly extended compared to the unforced case. It means that a developed stable vortex system is available for flow control purposes for a longer time.
Figure 10 shows that for *Case 1*,the vortex growth phase ranges from $t\approx1800$ to $t\approx4300$, i.e. for a period of $t_1=2500$. The corresponding flow topology at consequent stages during this phase is shown in Figure 11, patterns 2-5. For *Case 2*, the growth phase appears to be longer than in *Case 0* but shorter than in *Case 1*. It can be conjectured from Figure 12 that the growth phase starts at $t\approx1100$ and extends up to $t\approx3300$, i.e. covering a period of $t_2=2200$. The vortex structure is shown in patterns 2-4 of Figure 13.
The duration of the vortex growth phase in both thermally controlled cases is essentially larger than the reference value of $t_0=1800$. It shows that compared to the reference case (natural boundary layer development), the downstream distance of a developed and stably sustained vortical system extends by about 39% for the second harmonic forcing (*Case 1*) and by about 22% for the "irregular excitation" (). This effect is remarkable in a sense that a weak controlling factor causes noticeable changes of integral boundary-layer characteristics. It means (1) moderate heating requirements in either of the two cases, i.e. temperature of the stripes was raised only by an amount of $T= 3\,0K$above the (natural) adiabatic wall temperature, and (2) simplicity and flexibility of the control method itself.

In addition, the analysis of vortex patterns of the two controlled cases (Figures 11, 13) shows gradual transformation of the initially generated flow structures to larger scales, corresponding to the fundamental wavelength. Since equal simulation flow times are considered here, it can be concluded, that an excitation scheme strongly influences a near-wall region and the early vortex formation process (or shortly downstream in similar spatial experiments). In a middle term (or moving downstream in experiments), the natural vortex scale prevails approaching the fundamental. Besides, *the rate of the vortex formation explicitly depends on a type of forcing*, or arrangement of the heated stripes, i.e. their regular or irregular distribution along z.

3.1.1. VORTEX BREAKDOWN --

All simulations show a finite life-time of the inherent streamwise vortex system that ends with a collapse, i.e. an extremely rapid breakdown of the vortices which does not contradict physical reality and experimental data. The evolution scenario looks universal with thoroughly analyzed and found to be very similar mode-behavior in all studied cases. Thus the obtained results enable to suggest a following breakdown mechanism.

A characteristic mode-evolution is observed during the vortex growth phase in either sets of mode diagrams (Figures 8, 10, 12): the m_2 and m_3 (spanwise and wall-normal momentum component)

modes come into an oscillatory regime, which eventually culminates in a spike signal and corresponding vortex collapse. In addition, the characteristic oscillation amplitudes are slowly increasing. It should me mentioned that all the other variables are not subject to such oscillations. The spike signals seen there are rather a reaction (coupling) to the spike primarily occurring in the m_2 and m_3 modes. Therefore it can be supposed that the breakdown originates in a sort of instability which is only very weakly coupled with the streamwise velocity (momentum) field.
Since the observed m_2 and m_3 amplitude oscillations grow towards the breakdown, one may conclude that it is related to the slowly changing vertical scale of the vortices in the vortex growth phase. This suggests a mode selection mechanism, depending on the flow scales as it happens in any typical hydrodynamically unstable situation. The early stage of the instability displayed in pattern 6 of Figure 11 shows inflexion of a narrow zone with strong negative velocity component between the vortices. The corresponding "mushroom-structure" (iso-contours of u-velocity), the evidence of nonlinearity, though clearly visible in pattern 5, acquires a slight S-shape too. Even at this moment, the original mushroom-structure of the initial, elongated vortices is still seen, though strongly S-deformed.

There are two main features differing vortical fields before and after the breakdown (compare patterns 10 and 8 of Figure 9, patterns 5 and 8 of Figure 11, patterns 4 and 6 of Figure 13):

a) vortices after breakdown are much more compact (more circular); their height is reduced to less than a third of the height before breakdown;
b) vortex pairs consisting of two adjacent counter-rotating vortices become asymmetric; one of the two grows in size and strength for the expense of another one.

It was observed that domination of a clockwise over anti-clockwise rotating vortex or vice versa is a matter of minor initial random perturbations (of the order of the computer round off error). During breakdown, the system flips over to one side and subsequently stays in this asymmetry. The process is supposed can be driven by pronounced inflexion-point-type hydrodynamic instability occurring locally at the vertical jet-like flow between the counter-rotating vortices extremely elongated before the breakdown.

The shown *possibility to extend the phase of self-sustained vortices using thermal forcing can be interpreted as an effect on the instability mechanism controlling the vortex system collapse.*

3.1.4. VORTEX SYSTEM POST-BREAKDOWN –

is the phase logically and practically defined by previous events. The collapsed and regenerated streamwise vortical system in a form of asymmetric compact vortices settles down rather to a "quasi-asymptotic" than to asymptotic state. This is illustrated in terms of the flow topology for *Case 1* in the patterns 8-23, Figure 9, as a long-time series of the vortex system modifications. Here, the bursts explicitly appeared in the mode-structure, are related to some momentary stretching of the vortices normally to the wall (patterns 12, 13 and 17, 18 of Figure 9). Burst development can be interpreted using patterns 10, 11, 12 of Figure 9, corresponding to simulation times $t=6325,\ 6900,\ 7475,$ respectively. Analyzing pattern 10, one can notice that the wall-directed stream-traces of the dominant vortex almost do not cross contour lines and therefore are almost unaffected by u-velocity gradient. Moreover, the path of a fluid particle on such part of a stream-trace is oblique, i.e. its vertical component is negligibly small as well as the resulting centrifugal force component directed normally to the wall. It means that no strong forces affect the vortex, therefore it is in a quasi steady state. Pattern 11, on the contrary, shows that in a later stage, the vortex stream-traces go along gradients of the u-velocity field (e.g. like in a region around $y=3.5,\ z=4$ of the low streamwise momentum zones). Under the resultant action of the force field, conditions for vortex amplification are fulfilled and the vortex stretches vertically by the vertical centrifugal forces. These forces tend to restore the normally elongated, large vortical structure (like a reverse breakdown process).

However, well-pronounced asymmetry (and its underlying instability mechanism) breaks normal vortex growth; as a result, the vortex falls back into the calm and compact stage. This dynamic balance between centrifugal (body) force and instability mechanisms yields the repeatedly observed

events of breakdown splashes of variable parameters exposed in Figures 8, 10, 12 which were shown can be influenced due to the interference into the instability mechanism.
As a by-product of the burst events, some vorticity is shed into the free-stream.

Presented interpretation of the long-term observation of a developing streamwise vortical system can also explain the above mentioned characteristic time scales. In the post-breakdown phase, the *long time scale* is a time interval to turn-over the low-momentum fluid so that the conditions of vortex amplification under body force are fulfilled. The *short time scale* may be connected to the hydrodynamic instability, which tends to destroy normally-stretching, low-momentum-zone (note, that in patterns 12 and 18 of Figure 9 this elongated zone has got a local S-shape as described in the vortex breakdown scenario).

Revealed peculiarities of the flow topology and mode behavior drawn from numerical simulation should be verified and supplemented by experimental results to assist a deeper insight into the forced vortex dynamics of boundary-layers with embedded regular large-scale vortices. As for computational results, various presentations of the measured data are necessary to formulate the fundamental grounds of efficient ways of the flow control. These are first of all spanwise velocity profiles that proved to be very informative for the phenomena under consideration and spectral characteristics of boundary layers with available LSES.

3. 2. Thermal excitation of streamwise vortices -- experiment

Flow fields taking place around operating units in practice are far from the idealized numerical or laboratory conditions where types and values of disturbances introduced in a boundary layer are strictly defined and dozed. To approximate reality and to consider applicability of the thoroughly analyzed above thermal flow control method, it was tested experimentally under additional influence of other factors given by the surface compliance that is independent of thermally introduced effects.

Experiments were carried out in a water channel over its concave bottom with a 1 m long compliant test section where flush-mounted electrically heated thin wires were distributed regularly along z (Figure 6, position 3). Surface properties are known to damp any near-wall disturbances. Therefore it must be very demonstrative to see a combined effect of a generally mild $\Delta T(z)$ influence and that of the compliant surface (a coating was 0.6 mm sheet of a porous resin-type material with visco-elastic properties described in [35]). Three values of temperature T were used in the experiments corresponding to electric power applied, P_1=0 (no influence), P_2 =7.8 W and P_3=12.2 W. The $\Delta T(z)$ control effect was registered at two distances from the wall, y=2 and 3 mm. shown accordingly in left and right pattern sets of Figure 14. Flow-field visualization in xz-plane provided very sensitive and convenient $U(z)$ characteristics to estimate a boundary layer response to certain excitation and, subsequently, to choose the control parameters.

(a) The first patterns of both sets, $U(z)$ velocity profiles visualized just upstream of the "striped" test section, show floating in time $U(z)$ shape that can be interpreted as an evidence of the started meandering motion or as strongly unsteady behavior of large-scale streamwise vortices naturally developing in a transitional boundary layer.

(b) The available z-periodic mechanical properties of the surface (due to rigid longitudinal wires implanted in the compliant basement) stabilize the $U(z)$ velocity distributions at different distances from the surface hampering the naturally developing meandering motion in the boundary layer; however the amplitude of $U(z)$ stays large enough characterizing a significant rate of transition to turbulence. Besides, the spanwise periodicity of visco-elastic properties of the wall appears to be not a sufficient boundary condition to introduce a given smaller-scale, λ_g=1.2 cm, vortical structure in a boundary layer.

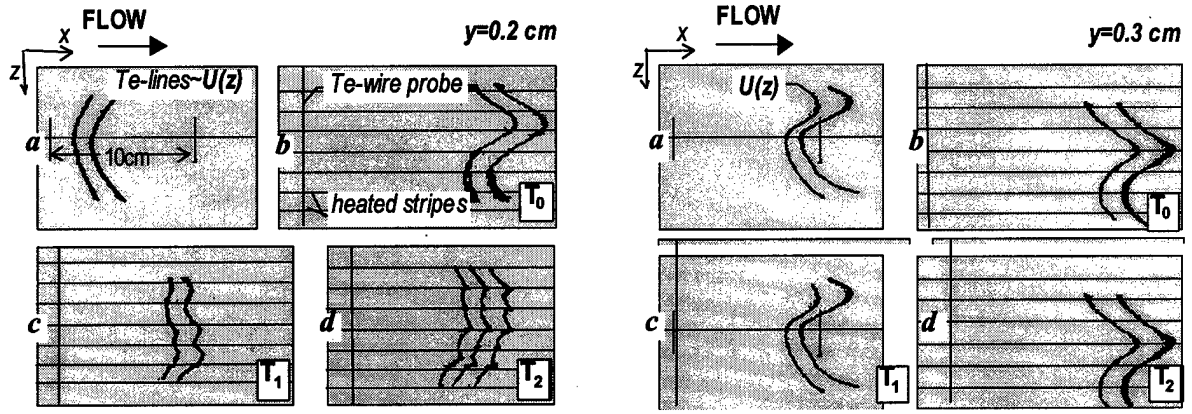

Figure 14. Visualization of a boundary layer over a concave surface controlled by the heated stripes, $Re\sim10^5$, G_g=2 (U_0 =5 cm/s, x=2.18 m; R=12 m);
y=2 mm (left set); y=3 mm (right set);

a: natural development of transition; **b-d**: excitation of longitudinal vortices, λ_g=1.2cm:
b – unheated stripes, $T=T_0$ =20°C; ***c***, ***d*** - heated stripes: $T_2 > T_1 > T_0$

(c) Moderate heating (corresponding to the value of electric power P_1=7.8 W) straightens the $U(z)$ velocity profiles which can be interpreted so that the transition rate decreases here compared to the undisturbed case. However visualized flow patterns show yet almost twice larger spanwise scale of the developing vortical structure than one induced there by the heated stripes, i.e. λ_z=2.4 cm=2λ_g.

(d) Growth of ΔT due to the stronger heating (P_2=12.2 W) keeps the averaged $U(z)$ profile straightened along a whole length of the control section and downstream; in addition, it induces the smaller-scale vortical structure according to the scale given by the stripes. It should be noted, that while being noticeable in the vicinity of the wall (y=2 mm), it transforms into a larger scale structure in the outer part of the boundary layer (for comparison, see patterns of Figure 3, **c**, left and right sets).

A tendency of the forced small-scale structure to grow is well observed both numerically and experimentally for all considered modes generated in a boundary layer, i.e. for nondimensional vortex scales Λ<240. However the life-time of incoming (or generated by any means) small-scale vortices, or their self-sustaining ability, depends very much on the spanwise scale of the forcing factor correlated with the basic flow parameters. It is well seen from comparison of the two numerically considered cases: (1) excitation of the pure second mode, Λ_2=84, and (2) a slightly "incorrect" excitation of Λ_2 that assumed the induced spectrum including the first, most amplified, mode. In spite of the constant boundary condition imposing the permanent preference to a given vortex scale, this forcing cannot prevent from the development and final dominance of a larger scale vortical structure. In addition, the initially prevailing second harmonic in the latter case gives up almost immediately to the first one; as a result, the growth phase of the vortex evolution shortens and the breakdown of the vortical system happens much faster.

The demonstrated results show that choosing the values of parameters, such as ΔT and λ_g, one can get an intended effect in a boundary layer: the prolonged, low-rate vortex field development with stabilized smoothed velocity profiles or direct generation of streamwise vortices with a given scale, moderate long-term or well-pronounced short-term effects.

3. 3. Spectral response of transitional and turbulent boundary layers to generated vortical structures

Kinematic portrait of a boundary layer with evolving streamwise vortices in a form of flow topology and velocity field transformation downstream and normally to the surface is not complete unless it is supplemented with its spectral characteristics. In this connection, standard procedure using fast Fourier transform was applied to recorded hot-wire signals and yielded the results presented in Figure 16. Legend for the experimental conditions of vortex generation is given in Table 1. Here y is a distance of a hot-wire probe over a surface, y_{vg} is a normal size of vortex-generators, is δ_1 a displacement thickness, δ is a boundary-layer thickness.

Table 1

	(a)	(b)	(c)	(d^1)	(d^2)	(e^1)	(e^2)
λ_g, cm	1.2	1.2	0.8	1.6	1.6	1.2	1.2
U_0, m/s	9.3	22.0	19.0	9.8	21.0	20.0	56.0
y_{vg}/δ_1	1.75	1.17	1.39	1.9	1.62	2.02	1.22
y/δ_1	2.0	1.33	1.01	1.38	1.18	1.03	0.615
y/δ	0.25	0.2	0.2	0.25	0.286	0.2	0.091

Streamwise vortices were induced in a boundary layer using vortex-generators of three sizes as it was mentioned above: spectral curves (a) and (b) were obtained with a smallest size, (c) and (d) – with a medium size, (e) – with largest vortex-generators. Accordingly, initial intensity of introduced disturbances was different since the vortex-generators interacted differently with a boundary layer what is seen from different y_{vg}/δ_1 values presented in Table 1. The (a) – (d) measurements were made in a transitional boundary layer while the (e^2) curve shows a reaction of a turbulent boundary layer to generated streamwise vortices. Reference spectral curves measured at two different distances from a wall are shown in Figure 15 for transitional (1, 2) and turbulent (3, 4) boundary layers. Their

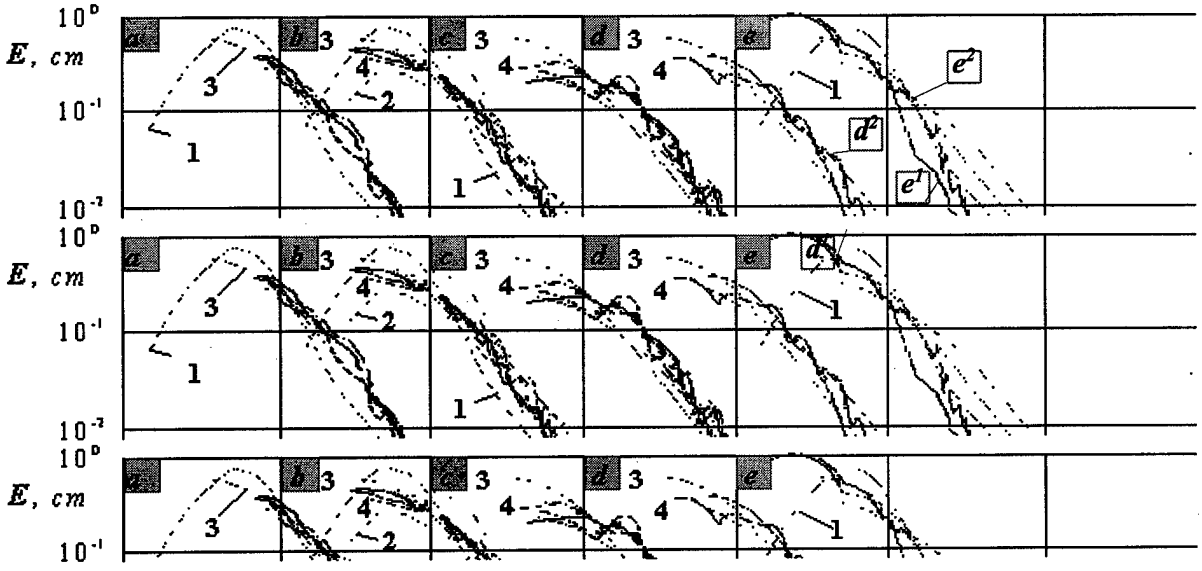

Figure 15. Power density spectra of u'-velocity fluctuations in a boundary layer:
1-2 – reference curves for natural laminar-turbulent transition, Re~10^5, y/δ_1=1.08 (1), y/δ_1=0.253 (2);
3-4 – reference curves for a turbulent boundary layer, Re~10^6, y/δ=0.21 (3), y/δ=0.063 (4);
for cases of generated streamwise vortices of different intensity (a-d), see the legend in the text.

comparison can bring to a conclusion that large-scale vortical structures naturally developing during laminar-turbulent transition redistribute energy along the spectrum in favor of its long-wave interval ($\alpha \approx 0.5$), significantly diminish intensity of fluctuations in the inertial interval ($0.5<\alpha<20$) and give rise to dissipative small-scale structures ($\alpha>20$).

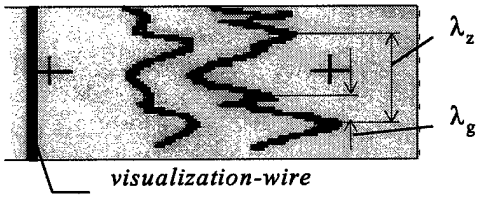

Figure 16. Visualized spanwise U(z) velocity profile: small-scale generated structure λ_g riding on a large-scale natural one λ_z

Spanwise velocity profiles (as a sensitive indicator of embedded streamwise vortices [26, 28] were registered at the same flow and control (vortex-generation) parameters. In case (a), influence of the vortex-generator array has shown a negligible effect on a boundary layer mean flow and increased fluctuation velocities. Therefore spectral curves have no very distinct features staying rather close to the "transitional" reference curve 1. However in the inertial spectrum interval, they approach the "turbulent" reference 3 curve though slightly sagged. Increased free-stream velocity with the same values of other parameters of the series (b) did not change the spectral pattern drastically. However closer similarity with the turbulent reference case can be mentioned here with less pronounced sag of the curves in the area between inertial-dissipative vortex scales. It can be interpreted as an evidence of a greater dismatch of the λ_g scale of generated vortices with the basic flow parameters (double value of the free-stream velocity compared to the previous case). In addition, the similarity with the turbulent spectrum is better seen when the results of measurements downstream of the vortex-generation array are compared with the turbulent reference curves obtained closer to the wall, i.e. in the region with statistically dominating smaller scale vortices. These flow conditions correspond to the stage of naturally developed streamwise vortices in a transitional boundary layer. Controlled excitation of smaller scale vortices under conditions of naturally existing structures results in energy redistribution in a boundary layer or in a more uniform spectrum (without a sag in the inertial interval which is well seen in the reference spectra 1 and 2 for a transitional boundary layer). In such cases, visualized U(z) velocity profiles look like a smaller scale wave riding on a large scale one (Figure 16).

In spectral terms, different boundary layer receptivity to generated vortices can be seen in (c) and (d) series of measurements downstream of the medium size vortex-generators. Twice smaller scale of generated vortices in case (c) compared to (d) causes an effect of turbulization mentioned for cases (a) and (b) when the spectrum is smoothed in its inertial and dissipative intervals being in a good agreement with the turbulent reference curve obtained closer to the wall. However separate peaks are observed, e.g. at $\alpha \approx 2.5$ (c). Figure 17 shows a mean flow response in a form of *U(z)* velocity profiles to twice differing scales of generated vortices. The upper pattern, similarly to Figure 16, represents two superimposed waves of generated small-scale λ_g and naturally developing large-scale λ_z vortices at the considered transition stage. The lower pattern demonstrates adequate reaction of the boundary layer to introduced vortices due to their parameters matched with the basic flow parameters.

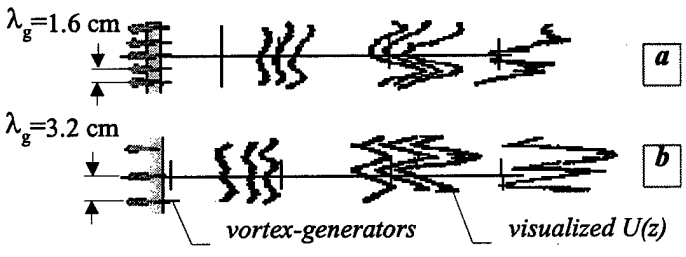

Figure 17. Flow-field response to twice differing scales of generated streamwise vortices similar to spectrally described (c) and (d) cases, "forced" laminar-turbulent transition

The latter case (Figure 17, b) is described in a spectral domain by a typical shape of curves with deep sags in the inertial interval up to short-wave dissipative one for both free-stream velocity values (see Table 1, cases d^1 and d^2). It can be interpreted in a way that available

embedded streamwise vortices that are maintained by the flow under given conditions suppress certain vortical scales in the boundary layer. This feature is displayed most strikingly in case (e), Figure 15, of a vortical field measured downstream of large-size vortex generators, i.e. in case of well established organized vortical structure. Explicit redistribution of energy between spectrum components occurs in favor of dominating LSES; it forms the mentioned sags within $1<\alpha<30$ of spectral curves both in the transitional (curve e^1) and turbulent (curve e^2) boundary layers.

More practically interesting case of a developed turbulent boundary layer proved to be flexible for manipulations too. The obtained sagged shape of its spectral e^2 curve is characteristic to the transitional boundary layer (curves 1, 2) showing deep changes in vortex dynamics. To some extent, this fact can be interpreted as certain relaminarization of a turbulent boundary layer with dominating deterministic vortical structure. In its turn, it enables to apply ideas and methods of the flow control tested for laminar/transitional boundary layers (e.g. approaches based on the stability and receptivity analysis)

Thus the analysis of the spectrum evolution during natural laminar-turbulent transition and spectral reaction of boundary layers to generated streamwise vortices can be summarized as follows.

Streamwise vortices embedded in a boundary layer display themselves in a spectral domain as an emphasized long-wave part of the spectrum for the expense of the inertial one. It is seen as a characteristic sagged shape of spectral curves (typically within $7<\alpha<15$) exhibiting the presence of large-scale vortices, no matter how they appeared -- in a process of natural laminar-turbulent transition or due to the generation in accordance with basic flow parameters so that they can be maintained in a boundary layer.

The directly found flow topology and its evolution after the vortical system generation are in a good agreement with the discussed above spectral patterns: both kinds of the fluid motion description evidence its growing scales in a boundary layer with embedded streamwise vortices.
These fundamental results should be taken into account for modeling of near-wall flows with LSES, for control of laminar-turbulent transition and transport processes near a wall. In particular, they can help to determine parameters of vortices (correlated with basic flow parameters) sustained longer after they have been generated in a boundary layer.

4. Conclusions

Flow control similarity principle was formulated as a basis for optimal management of boundary layer characteristics: generation of a vortical structure type similar to one intrinsically dominating in the flow with parameters and intensity correlated with basic flow parameters and with a boundary-layer control objective.

Streamwise vortices were shown to be one of such structures inherent to boundary layers affected by body forces. On the one hand, such flows are interesting and important to study from the viewpoint of applications since in practice, flow dynamics almost always is driven by body forces (one of the examples is a flow around a turbine blade subjected to centrifugal and buoyancy forces). On the other hand, being a deterministic fluid motion, the streamwise vortices can be described in the frame of stability analysis; therefore the flow control mechanisms can also be analyzed and formulated in deterministic terms. Fundamental analysis of the vortex dynamics helped to find focal points to interfere its basic processes to maintain a flow structure of preferred type and scale.

It was shown that generally, the optimal control means the interference into the instability mechanism of a vortical motion developing under centrifugal forces. High shear layers between the streamwise vortices appeared to be a critical zone for originated instability of the vortical system. Therefore it is

most efficient to apply any control techniques at a moment (or at the Reynolds number) corresponding to the vortex growth phase remarkable for its well-developed stable vortices. Such intervention should limit vortex normal-to-wall growth rate and accordingly, the development of a high shear layer as a source of instability leading the settled structure to breakdown.

This conclusion is supported by combined spectral / velocity-field / topological analysis of the boundary layer with embedded (naturally developing or generated and further evolving) streamwise vortices. Obtained experimental and numerical results are in a good agreement having revealed typical characteristics and response of a boundary layer to generated streamwise vortices:

- growing scales of the dominating vortical motion both downstream and normally to the surface;
- mode competition in favor of definitive prevalence of a large-scale fundamental even under condition of a constant different-scale forcing from the wall;
- controllable growth rates and amplitudes of all basic flow variables owing to different applied vortex excitation schemes;
- non-zero receptivity of both transitional and turbulent boundary layers under centrifugal forces to induced streamwise vortices;
- power spectra redistribution in favor of a long-wave interval in transitional and turbulent boundary layers with embedded streamwise vortices;
- formation of a stable regular flow structure in a near-wall region under conditions of "impure" fashion of the vortex-generation (over compliant coatings which tend to damp any effects);
- correlation between ΔT (or a height of vortex generators) and λ_g to obtain a required vortical system in a boundary layer.

The demonstrated method to control vortex growth rates can be used either to stabilize the flow situation (delaying laminar-turbulent transition) or to intensify mixing processes near the wall and thus postponing flow separation or enhancing heat transfer.
In addition, a possibility was shown to choke energy of turbulent fluctuations in a long-wave spectrum interval, i.e. to expose and express the observed effects in terms typical for turbulence description. It implies prospects to further extend the experience of the transitional boundary-layer control to turbulent flows using both obtained results and well developed methods of turbulence investigation. This conclusion defines concrete tasks for future investigations focused on new technology requirements, i.e. on detailed analysis of the favorable turbulent boundary-layer structure formation and maintenance. The formulated similarity principle can be used a guiding idea to control turbulent flows affected by body forces.

References

1. Alekseenko, S.V., Bilski, A.V., Markovich, D.M., Semenov, V.I. Sensitivity of impining turbulent jets to external disturbances. *Proc. Eleventh Symposium on Turbulent Shear Flows. Sep.8-11, 1997, Grenoble, France.* Vol. 2, pp. 22-18—22-23.
2. Alekseenko, S.V., Bilsky, A.V., Markovich, D.M., Semenov, V.I. Evolution of instabilities in an axisymmetric impinging jet. *Proc. of 4th Int. Symp. on Engineering Turbulence Modeling and Measurements, May 24-26, Corsica, France*, 637-645, 1999.
3. Blackwelder, R. F. Analogies between transitional and turbulent boundary layers, 1983, *Phys. Fluids* **26** (10), 2807.
4. Blackwelder, R.F. Coherent structures associated with turbulent transport, in M.Hirata and N.Kasagi (ed.), 1988, *Transport Phenomana in Turbulent Flows*, Hemisphere Publ. Corp., 69-88.
5. Delfs, J., Yin, J., Li, X., Leading edge noise studies using CAA, 1999, AIAA Paper No. 99-1897.
6. Delfs, J.W., Yurchenko, N.F., Rivir, R.B., Vortex dynamics of boundary layers under body forces: dominating mechanisms and control, 1999, *Proc. Workshop "Cooperation between the Eur. and Sib. Scientists in a Field of Physical Hydromechanics"*, Novosibirsk, Russia.

7. Floryan, J. M. (1989) Goertler instability of boundary layers over concave and convex walls, *Phys. Fluids,* **29** (8), pp 2380-2387.
8. Ilyushin B. B., Kurbatskii A.F. Modeling of pollutant dissipation in convective atmospheric boundary layers. *Izv. RAN, Physics of atmosphere and ocean*, **32**, No. 3, 307-322, 1996. (in Russian)
9. Ilyushin, B. B. Modeling of inter-diffusion of turbulent fields with different scales. *Modeling in mechanics,* **4(21)**, No.4. 53-63, 1991. (in Russian)
10. Ilyushin, B.B., Kurbatskii, A.F. Modeling of turbulent transport in PBL with third-order moments. *Proc. Eleventh Symposium on Turbulent Shear Flows. Sep.8-11, 1997, Grenoble, France.* Vol. 2, pp. 2019-2024.
11. Jiang, N., Shu, W., Wang, Z-D. The maximum energy criterion for identifying burst events in wall turbulence using wavelet analysis, *Acta Mechanica Sinica.* 29, No.3, 406-412 (in Chinese), 1997.
12. Jiang, N., Wang, Z-D., Shu, W. Using wavelet transform to study the LIPSHCHITZ local singular exponent. *Applied Mechanics and Mathematics* (English Edition), 19, No.10, 983-990, 1998.
13. Laurien, E., Delfs, J., Bohnsack, E., A Spectral Method for the Numerical Simulation of Compressible Boundary-Layer Transition, 1993, *ZAMM* **73**, 5, T556-T559.
14. Lesieur M., Métais, O. New trends in large-eddy simulations of turbulence. Ann.Rev. Fluid Mech. 1996. Vol 26.
15. Métais, O., Lesieur, M. Spectral large-eddy simulation of isotropic and stably-stratified turbulence. J. Fluid Mech., 1992, **239**, 157-194.
16. Monin, A.S., Yaglom, A.M. Statistical Hydromechanics (Part 1,2). Moscow: Science, 1967.
17. Nagano, Y., Tagawa, M. Coherent motions and heat transfer in a wall turbulent shear flow. *J. Fluid Mechanics,* 305, 127-157, 1995.
18. Rivir, R. B., Transition on Turbine Blades and Cascades at Low Reynolds Numbers, 1996, 14th AIAA Fluid Dynamics Conference, New Orleans, *AIAA 96-2079*, June 1996.
19. Rivir, R.B., Sondergaard, Dalhstrom, Ervin, Low Reynolds Number Turbine Blade Cascade Calculations, 1996, *The Sixth International Symposium on Transport Phenomena and Dynamics of Rotating Machinery*, Honolulu, Hawaii, Vol. 2, pp. 132, February 1996.
20. Sabry, A.. S., Liu, J. T. C. Longitudinal vorticity elements in boundary layers: nonlinear development from initial Goerler vortices as a prototype problem, 1991, *J. Fluid Mechanics*, **231**, 615-663.
21. Saric, W. S. Goertler vortices, 1994, *Annu. Rev. Fluid Mech.*, **26**, 379-409.
22. Swearingen, J. D., Blackwelder, R. F. The growth and breakdown of streamwise vortices in the presence of the wall, 1987, *J. Fluid Mechanics*, **182**, 255-290.
23. Yurchenko, N. Power of beauty: streamwise vortices, *Proc. Science & Art Conference 2000, Zurich, 27 February – 3 March, 2000.*
24. Yurchenko, N. Receptivity of boundary layers under centrifugal forces, 2000, *8th European Turbulence Conference, Barcelona , Spain, June 27-30, 2000 (submitted).*
25. Yurchenko, N., Delfs J. Boundary layer control over an active ribleted surface. 1999. *Proc. IUTAM Symp. on Mechanics of Passive and Active Flow Control*, Goettingen, Germany, eds. G.E.A.Meier and P.R.Viswanath, Fluid Mecanics and its Applications, Vol.53, 217-222, Kluwer Acad. Publishers.
26. Yurchenko, N., Delfs J. Optimal control of boundary layers under body forces, *Proc. IUTAM Symposium on Laminar-Turbulent Transition, Sedona, U.S.A., September 13-19, 1999.*
27. Yurchenko, N., Rivir, R. Improvement of the turbine blade performance based on the flow instability and receptivity analysis, 2000, *8th Int. Symp. on Transport Phenomena and Dynamics of Rotating Machinery (ISROMAC-8), Honolulu, Hawaii, March 26-30, 2000.*
28. Yurchenko, N.F. Experimental technique to study longitudinal vortices in a boundary layer, 1981, *Engineering-Physical J.*, **41**, 6, 996-1002.
29. Yurchenko, N.F. Optimization of heat transfer control based on a receptivity approach, 1998, *Proc. Turbulent Heat Transfer Conference, Manchester, UK,* P72-P81.
30. Yurchenko, N.F., Babenko, V.V., Kozlov, L.F., Transition process under different disturbing factors, 1987, *Proc., IUTAM Symposium on Turbulence Management and Relaminarization, Bangalore, India*, 19-23.

31. Yurchenko, N.F., Delfs, J.W., Boundary layer control over an active ribleted surface, 1999. *Proc. IUTAM Symp. on Mechanics of Passive and Active Flow Control*, Goettingen, Germany, eds. G.E.A.Meier and P.R.Viswanath, Fluid Mecanics and its Applications, Vol.53, 217-222, Kluwer Acad. Publishers.
32. Yurchenko, N.F., Delfs, J.W., Nonlinear development of the forced vortical structure in flows under centrifugal forces. 1999, *11th International Couette-Taylor Workshop, Bremen, Germany, July 20th – 23rd, 1999.*
33. Yurchenko, N.F., Rivir, R.B. Flow management using inherent transition and receptivity features, 1998, *Proc. International Symposium on Seawater Drag Reduction*, Newport, USA.
34. Yurchenko, N.F., Zygmantas, G.P. Generation of longitudinal vortices in boundary layers affected by body forces, *Engineering-Physical J.*, 1989, **57**, 3, 392-398
35. Yurchenko, N.F. Compliant coatings for transitional boundary layer control, 1997, *Proc. AGARD Workshop on High-Speed Motion in Water*, pp 13.1-13.7, Kiev, Ukraine, Sept. 1997.
36. Zhou, H. The mechanism for the generation of coherent structures in the wall region of a turbulent boundary layer, 1995, *Science in China (Series A)*, **38**, 2, 188-198.